A new role for *Escherichia coli* Dam DNA methylase in prevention of aberrant chromosomal replication

Nalini Raghunathan[1,2], Sayantan Goswami[1,2,†], Jakku K. Leela[1,†], Apuratha Pandiyan[1] and Jayaraman Gowrishankar [1,*]

[1]Laboratory of Bacterial Genetics, Centre for DNA Fingerprinting and Diagnostics, Hyderabad 500039, India and
[2]Graduate Studies, Manipal Academy of Higher Education, Manipal 576104, India

ABSTRACT

The Dam DNA methylase of *Escherichia coli* is required for methyl-directed mismatch repair, regulation of chromosomal DNA replication initiation from *oriC* (which is DnaA-dependent), and regulation of gene expression. Here, we show that Dam suppresses aberrant *oriC*-independent chromosomal replication (also called constitutive stable DNA replication, or cSDR). Dam deficiency conferred cSDR and, in presence of additional mutations (Δ*tus*, *rpoB*35) that facilitate retrograde replication fork progression, rescued the lethality of Δ*dnaA* mutants. The DinG helicase was required for rescue of Δ*dnaA* inviability during cSDR. Viability of Δ*dnaA dam* derivatives was dependent on the mismatch repair proteins, since such viability was lost upon introduction of deletions in *mutS*, *mutH* or *mutL*; thus generation of double strand ends (DSEs) by MutHLS action appears to be required for cSDR in the *dam* mutant. On the other hand, another DSE-generating agent phleomycin was unable to rescue Δ*dnaA* lethality in *dam*+ derivatives (*mutS*+ or Δ*mutS*), but it could do so in the *dam* Δ*mutS* strain. These results point to a second role for Dam deficiency in cSDR. We propose that in Dam-deficient strains, there is an increased likelihood of reverse replication restart (towards *oriC*) following recombinational repair of DSEs on the chromosome.

INTRODUCTION

In the gamma-proteobacteria, adenine bases in the palindromic GATC sequences in DNA are N^6-methylated on both strands by the Dam DNA methylase [reviewed in (1–3)]. Discovered more than four decades ago (4,5), the enzyme catalyzes maintenance methylation on the daughter strands of the pair of hemi-methylated duplexes that are generated following semi-conservative replication of DNA, although it can also perform *de novo* methylation on duplexes in which both strands are unmethylated at these sites.

In *Escherichia coli* and *Salmonella enterica* serovar Typhimurium, Dam's action as a maintenance methylase *in vivo* defines a time window of hemi-methylation following passage of a replication fork when the parental and daughter strands can be distinguished by their GATC methylation status (6). This time window is then exploited by different replication-related processes in bacterial cells. Thus following recognition by MutS of replication errors, the MutH endonuclease cleaves the unmethylated daughter strand at GATC to initiate MutHLS-directed mismatch repair. Second, SeqA binds hemi-methylated GATC sequences to mediate multiple functions including sequestration of the site (*oriC*) for initiation of chromosomal DNA replication, transcriptional repression of the essential protein DnaA needed for replication initiation at *oriC*, and cohesion of sister chromatids in the wake of a progressing replication fork. Third, hemi-methylated GATC regions can also serve to control gene transcription and plasmid replication, by modulating the binding of specific proteins to the respective regulatory regions (1–3).

Several phenotypes of *dam* mutants are related to Dam's role in methyl-directed mismatch repair, and hence are suppressed by mutations in the *mutH*, -*L* or -*S* genes (7,8). The understanding is that, in absence of Dam function, mismatches generated during replication lead to double-strand ends (DSEs) engendered by MutH endonuclease at the unmethylated GATC sequences, and that such DSEs do not occur in the *dam mutH/L/S* derivatives (8). MutH has been shown *in vitro* to cleave both strands at unmethylated GATC sites (9). The phenotypes of *dam* mutants that are *mutH/L/S*-suppressed (and therefore believed to be consequential to DSE generation) include: synthetic lethalities with mutations in genes for recombinational repair of DSEs (*recA, -B, -C, ruvA, -B, -C*) and for replication restart (*priA, -B, dnaC*); sensitivity to 2-aminopurine and genotoxic agents; and hyper-recombination (1–3,8,10,11).

*To whom correspondence should be addressed. Tel: +91 40 27216122; Fax: +91 40 27216006; Email: shankar@cdfd.org.in
†The authors wish it to be known that, in their opinion, the second and third authors should be regarded as Joint Second Authors.

In this work, we have identified a novel function for Dam methylase, which is to control aberrant *oriC*-independent bacterial replication. In wild-type *E. coli*, replication of the circular chromosome is achieved by DnaA-mediated initiation at *oriC* of a pair of replication forks which then proceed bidirectionally to meet in the terminus region [reviewed in (12,13)]. The seven highly transcribed *rrn* operons are all oriented such as to be co-directional with fork progression on the two replichores. The terminus region is demarcated by the Tus protein-bound *TerA* and *TerC/B* sites which act as polar (unidirectional) barriers to fork progression, so that replication forks do not ordinarily progress into the opposite replichore, that is, towards *oriC* (13–16).

Aberrant *oriC*-independent chromosomal replication, also referred to as constitutive stable DNA replication (cSDR), has been described in *E. coli* derivatives harbouring mutations in *rnhA, recG* or *topA*, that encode RNase HI, RecG helicase and topoisomerase I, respectively (17–19); most recently, it has also been reported to occur in triple-exo mutant strains, that is, mutants simultaneously deficient for 3′-DNA exonucleases I, VII and SbcCD, or exonucleases I, VII and the 5′-DNA exonuclease RecJ (20). cSDR is critically dependent on the phenomenon of replication restart (17), which in turn is mediated by action of the PriA, PriB, PriC and DnaT proteins in loading of the DnaB replicative helicase at sites of initiation other than *oriC* (21–24). Increased occurrence of RNA-DNA hybrids or R-loops is believed to be responsible for cSDR initiation in *rnhA* and *topA* mutants (17,18), whereas for *recG* mutants several alternative models have been proposed in this regard: R-loops (17), aberrant replication initiation following fork collisions in the terminus region (25–27), continued replisome progression even after converging forks meet one another (28), and retrograde or reverse replication restart (24,29). A phenomenon related to cSDR is inducible stable DNA replication (iSDR), which is also dependent on replication restart mechanisms but unlike cSDR requires exposure of bacterial cells to DNA damaging agents (17,30).

One of the prominent genetic manifestations of cSDR is the rescue of lethality that is otherwise ordinarily associated with deficiency of DnaA (in other words, cSDR can compensate for loss of *oriC*-dependent replication in these situations). Such rescue has been demonstrated in *rnhA, recG* and triple-exo mutants (17,20,25–27). Completion of chromosome duplication by cSDR under these conditions entails that two kinds of obstacles be overcome (13): (i) Tus-bound *Ter* barriers, and (ii) transcription-replication conflicts, especially at *rrn* operons. Thus, mutations which help mitigate these impediments—Δ*tus* for the former (13–16), and *rpoB*35* encoding an altered RNA polymerase for the latter (31–33)—are either required for (in case of *recG* or triple-exo mutants) or greatly facilitate (in case of *rnhA*) the suppression by cSDR of lethality caused by loss of DnaA function (20,25–27).

We now report that Dam deficiency also confers cSDR, and that Δ*dnaA* inviability is suppressed by Δ*dam* in presence of the Δ*tus* and *rpoB*35* mutations. Furthermore, as has been reported earlier for *recG, rnhA, topA* and the triple-exo mutants (19,20,25–28,34), *dam* derivatives that are *dnaA+* exhibit a prominent 'mid-terminus' peak in DNA copy number analysis which is an apparent signature of cSDR. Suppression of Δ*dnaA* lethality by Δ*dam* was affected by *mutH/L/S* mutations, suggesting that DSEs are required for cSDR in the Dam-deficient strains. At the same time, our data indicate that Dam deficiency also plays a second role in cSDR, which we propose is in facilitating reverse restart of replication forks on the chromosome.

MATERIALS AND METHODS

Growth media and bacterial strains

The growth media were LB and 0.2% glucose-minimal A (35), the latter supplemented with auxotrophic requirements as appropriate and with Casamino acids at 1% where indicated. Unless otherwise indicated, the growth temperature was 37°C. L-Arabinose (Ara), Xgal, tetracycline (Tet), kanamycin (Kan), ampicillin (Amp), chloramphenicol (Cm) and trimethoprim (Tp) were used at concentrations described previously (36); supplementation with spectinomycin or the various genotoxic agents was at concentrations as mentioned elsewhere in the text. Genotypes of *E. coli* strains are listed in Supplementary Table S1, with the following knock-out (Kan^R insertion-deletion) alleles sourced from the collection of Baba *et al.* (37): *dam, tus, mutH, mutL, mutS, seqA, dinG, rnhA, recG, recA, rdgB, sulA, metF* and *argE*.

Plasmids

Previously described plasmids include (brief description for each in parentheses): pCP20 (Amp^R Cm^R, pSC101 derivative carrying Flp recombinase) (38): pBAD18 (Amp^R, vector for Ara-induced expression of genes cloned downstream of P*ara*- promoter) (39); pMU575 (Tp^R, single-copy-number vector with *lacZ+*) (40); pASKA-*dam+* and its corresponding empty vector pCA24N from the ASKA collection (41) (Cm^R, former expresses Dam methylase); and pAD16 (Amp^R, expressing ParB::YGFP protein, that is, a fusion of ParB with a variant green fluorescent protein) (42). The details of construction in this study of plasmids pHYD2388, pHYD4805, and pHYD5701 (pMU575 derivatives carrying *S. enterica* genes *dnaA+*, *dnaA+ recG+*, and *recA+*, respectively) and of plasmid pHYD4807 (pBAD18 derivative carrying *E. coli mutS+*) are described in the *Supplementary Text*.

Genetic methods

Procedures for P1 transduction (43) and transformation (44) were as described. Recombineering of Δ*dnaA*::Kan was by the method of Datsenko and Wanner (38), as described in more detail in the *Supplementary Text*. Site-specific deletion of FRT-flanked Kan^R cassettes was achieved with the aid of plasmid pCP20, as described (38). The *polA12* allele was introduced by cotransduction with a linked Kan^R marker (45); procedures for introduction and testing of alleles *rpoB*35* and *priA300*, and for crossing out of phi80 prophage, are detailed in the *Supplementary Text*. Presence or absence in strains of phi80 prophage was tested by duplex-PCR with a set of three primers as earlier described (46).

To achieve Ara-induced RNase HI overexpression, a P$_{ara}$-*rnhA* construct was used that had previously been transferred (36) from a pBAD18-derived plasmid to the λ *att* site on the chromosome by the method of Boyd *et al.* (47); the same method was used to construct chromosomal integrations at the λ *att* site of the P$_{ara}$ promoter alone from the pBAD18 vector (as negative control), and of a P$_{ara}$-UvsW construct from the plasmid pHYD2368 that has also been previously described (36).

For scoring rescue of Δ*dnaA* lethality, cultures of the Δ*dnaA* derivatives carrying pHYD2388 were grown overnight in Tp-supplemented medium and plated at suitable dilutions on Xgal medium without Tp. Typically for strains in which Δ*dnaA* was lethal, the proportion of white colonies to total was <0.2%. Rescue of lethality was taken to be robust if (i) white colonies were obtained at >5% of the total, and (ii) these colonies could be maintained indefinitely by sub-culturing on the same medium.

Tn*10* stability and pCP20 transformation in *dam* mutants

dam derivatives carrying *btuB*::Tn*10* yielded spontaneous Tet^S derivatives at high enough frequency to comprise ∼20% of cells in a culture, indicative of derepression of IS*10* transposition in the mutants (48); these strains were therefore routinely tested for their Tet^R phenotype before use in experiments.

We also discovered in this study that plasmid pCP20, and other pSC101 derivatives, fail to yield transformants in a *dam* strain but are able to transform a *dam seqA* mutant; furthermore, plasmid preparations made from the latter now yielded transformants even in the *dam* strain. These results indicate for the first time that pSC101 also belongs to that category of replicons in which a Dam-methylated template is converted to hemi-methylated DNA in the *dam* mutant following one round of replication, and is then irreversibly bound by SeqA to stop further replication (49).

Copy number analysis by deep sequencing

In the initial experiments for copy number analysis, genomic DNA was extracted from cultures grown in LB to mid-exponential phase ($A_{600} \approx 0.4$) with the aid of a commercial kit (PureLink; Invitrogen, USA). It is now known that such preparations are depleted of DNA from the *rrn* operon regions (50,51), and therefore in subsequent experiments we prepared genomic DNA from cultures by phenol-chloroform extraction, as described (44).

Deep sequencing was performed on Illumina HiSeq platforms with a paired-end sequencing strategy, to achieve ∼100-fold coverage for each preparation. Sequence reads (each 100 or 250 bases long) were subjected separately to *de novo* contig assembly as well as to alignment to reference genomes (either strain MG1655, or MG1655 with phi80 prophage); the aggregate base read counts for each culture (after alignment to MG1655) are given in Supplementary Table S2.

The aligned sequence data were then used for copy number determinations (by a moving-average method), and for mutation detection, as described in the *Supplementary Text*. The copy number of each genomic region was represented

on a semi-log graph as an 'enrichment ratio', which is defined as the ratio of (i) the base read count for that region in an exponential-phase culture (normalized to the aggregate of aligned base read counts for that culture) to (ii) the base read count, similarly normalized, for the same region in a stationary-phase culture (where all regions are expected to be equally represented).

cSDR detection by flow cytometry and fluorescence microscopy

For assessment of cSDR by flow cytometry, the method was essentially that described by Martel *et al.* (52), involving treatment of cultures in exponential phase in LB with 400 µg/ml of the protein synthesis inhibitor spectinomycin for 2 h, followed by addition of the nucleotide analogue EdU (0.08 mM) for 1 h. Cells were fixed with 3.7% paraformaldehyde for 30 min at room temperature, and then permeabilized and treated with Alexa Fluor-488 conjugate as described (52). Flow cytometry was performed on the BD-FACS Aria III platform, and data (for 10 000 cells in each preparation) were analyzed with BD-FACS Diva software (version 6.0).

For *parS* copy number detection by fluorescence microscopy (42,53), cultures (of strains bearing *parS* integrated near the chromosomal terminus region and expressing ParB::YGFP constitutively from plasmid pAD16) were grown to early exponential phase ($A_{600} \approx 0.4$) at 37° in 2 ml of glucose-minimal A; one-half of each was treated with spectinomycin at 400 µg/ml for 2 h while the other half was stored on ice for this period. Cells from each of the aliquots were then washed twice in equal volumes of phosphate-buffered saline (PBS) (44), resuspended in 0.5 ml of PBS, and visualized under 60× magnification through a fluorescence microscope (DeltaVision OMX V3, GE Healthcare) at excitation and emission wavelength settings of 488 and 528 nm, respectively. Raw images were processed with the aid of ImageJ software (version 1.52i).

Other methods

The protocols of Sambrook and Russell (44) were followed for DNA manipulations and analysis. Immunoblotting with S9.6 monoclonal antibody for detection of RNA–DNA hybrids was as described (54). For phase contrast microscopy, cells were cultured in glucose-minimal A to mid-exponential phase, washed with PBS and resuspended in PBS; they were then layered atop 1% agarose pads on slides and overlaid with coverslips for viewing under 100× magnification on a Nikon Eclipse 80i microscope, and images were analyzed with the aid of NIS-Elements D3.0 software.

RESULTS

Dam deficiency is associated with cSDR

Given the occurrence of MutHLS-generated DSEs in *dam* mutants, as well as the similarities that exist between iSDR and cSDR, we examined whether cSDR occurs in Dam-deficient strains. Two different assays were employed, with the common feature being detection of continuing DNA synthesis following complete cessation of *oriC*-initiated

A
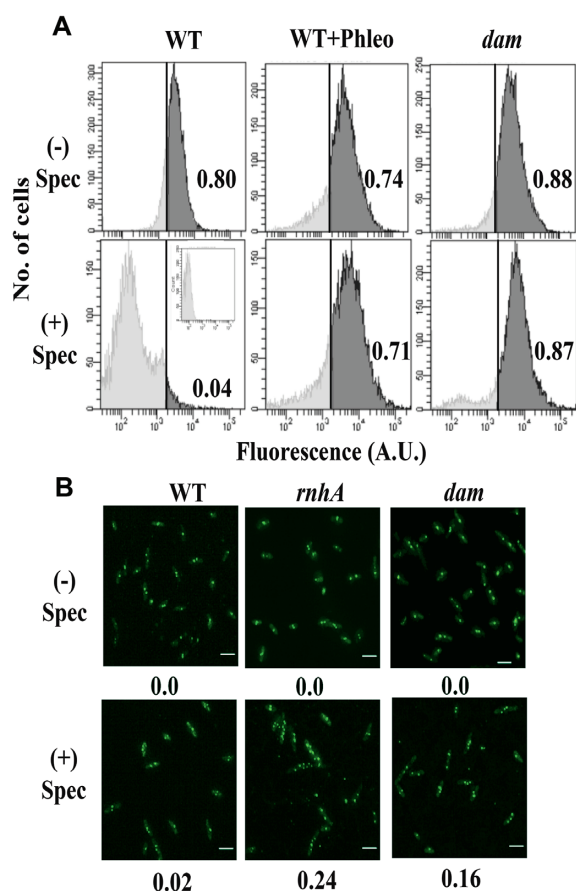
Figure 1. cSDR in *dam* mutants. (**A**) Analysis by flow cytometry, as described (52), of DNA synthesis in cultures of (i) parental (WT) strain GJ18609, (ii) WT with phleomycin (WT+Phleo) at 1 μg/ml, and (iii) the isogenic *dam* mutant GJ16494 (*dam*), without (–) or with (+) treatment with spectinomycin (Spec). In each panel, the proportion (of the total) of cells in which the fluorescence value exceeded the gating threshold (vertical line) is given at right. Inset within bottom left panel depicts fluorescence in cells exposed to neither EdU nor Alexa Fluor 488 (that is, autofluorescence). (**B**) Fluorescence microscopy for detection of ParB::YGFP-*par*S foci in cells from cultures of plasmid pAD16-bearing derivatives of parental (WT) strain GJ15830 and its isogenic *rnh*A or *dam* mutants (GJ15831 and GJ15832, respectively) without (–) or with (+) treatment with Spec. Beneath each panel, the proportion of cells with >2 foci is indicated (minimum of 300 cells examined). Scale bar, 3 μm.

replication. Such cessation was achieved by treatment of cultures for 2 h with the protein synthesis inhibitor spectinomycin (52), since it is known that each round of replication initiation at *oriC* requires fresh synthesis of DnaA, and that all replication forks which were previously initiated from *oriC* would have progressed to completion within this period.

In the first assay involving flow cytometry, DNA synthesis in individual cells of cultures was analyzed by fluorescence detection of incorporation of the nucleotide analog EdU before and after spectinomycin addition, as described earlier (52). In the spectinomycin-treated cultures, whereas just 4% of cells in the wild-type strain exhibited new DNA synthesis that exceeded the fluorescence gating threshold of 2×10^3 units, 87% of the Δdam mutant cells did so, indicative of cSDR (Figure 1A). Around 70% of cells in a culture

of the wild-type strain exposed to sublethal concentration (2 μg/ml) of the radiomimetic agent phleomycin, which generates DSEs (55,56), also exhibited continued DNA synthesis exceeding the gating threshold following spectinomycin treatment, indicative of iSDR (Figure 1A).

For the second assay employing fluorescence microscopy, the number of foci of ParB::YGFP-bound *parS* was counted in individual cells of strains in which *parS* had been integrated near the chromosomal terminus region (42,53). The expectation was that normal cells would harbour at most two foci following spectinomycin addition, whereas those exhibiting cSDR would display a substantial proportion with multiple (>2) foci (since DnaA- and *oriC*-independent replication would lead to additional copies of *parS* in these cells); this expectation was confirmed with cultures of the wild-type strain and the *rnhA* mutant, respectively (Figure 1B). Cells of the Δdam mutant also behaved like the *rnhA* derivative and showed an increased proportion of multiple foci in this assay (Figure 1B). We conclude that Dam deficiency is a new example of a perturbation that confers cSDR in *E. coli*.

Rescue of Δ*dnaA* lethality by Dam deficiency in presence of Δ*tus* and *rpoB*35 mutations

Based on the findings above, we tested whether cSDR conferred by the *dam* mutation could restore viability in DnaA-deficient strains. In earlier studies (17,20,25–27,34), the temperature-sensitive *dnaA46* mutation had been employed, and hence cSDR-mediated rescue of lethality could only be assessed at 42°. In this work, we chose to use $\Delta dnaA$ for the genetic studies on cSDR, and adopted a strategy analogous to those employed by us earlier to study rescue of knockout lethality in other essential *E. coli* genes such as *rne*, *rho* or *nusG* (36,54,57).

We constructed strain GJ16459/pHYD2388 (as described in Materials and Methods) with $\Delta dnaA$ and Δlac mutations on the chromosome, and a single-copy-number Tp^R shelter plasmid carrying functional copies of *lacZ* and *dnaA* from, respectively, *E. coli* and *S. enterica*. This strain and its derivatives grow as blue colonies on Xgal-supplemented plates; they also generate spontaneous plasmid-free segregant cells at a frequency of ∼5–15% which, however, can only grow and be subcultured as white colonies on Tp-free Xgal medium if they carry mutation(s) that rescue Δ*dnaA* lethality. Strain GJ16459 also carries the *rpoB*35 and Δ*tus* mutations in order to facilitate the progression around the chromosome of cSDR-initiated forks across, respectively, the sites of transcription-replication conflict (especially at *rrn* operons) and the *Ter* sequences in the terminus region (20,25–27). We used the *rnhA* and *recG* mutations as positive controls (17,25–27) to confirm their ability to confer viability in absence of DnaA function (Figure 2, compare panels ii and iii with panel i).

Two different null alleles of *dam* (Δ*dam*::Kan, and *dam*::Tn9) rescued the Δ*dnaA* lethality in this assay done at 37°C (Figure 2, panels iv–v), which did not occur in the derivative that was *tus*$^+$ *rpoB*$^+$ (Figure 2, panel xii). The phenotype was most prominently exhibited on nutrient-rich media [LB (Figure 2), or minimal A supplemented with Casamino acids (Supplementary Figure S1, panels i–iii)]
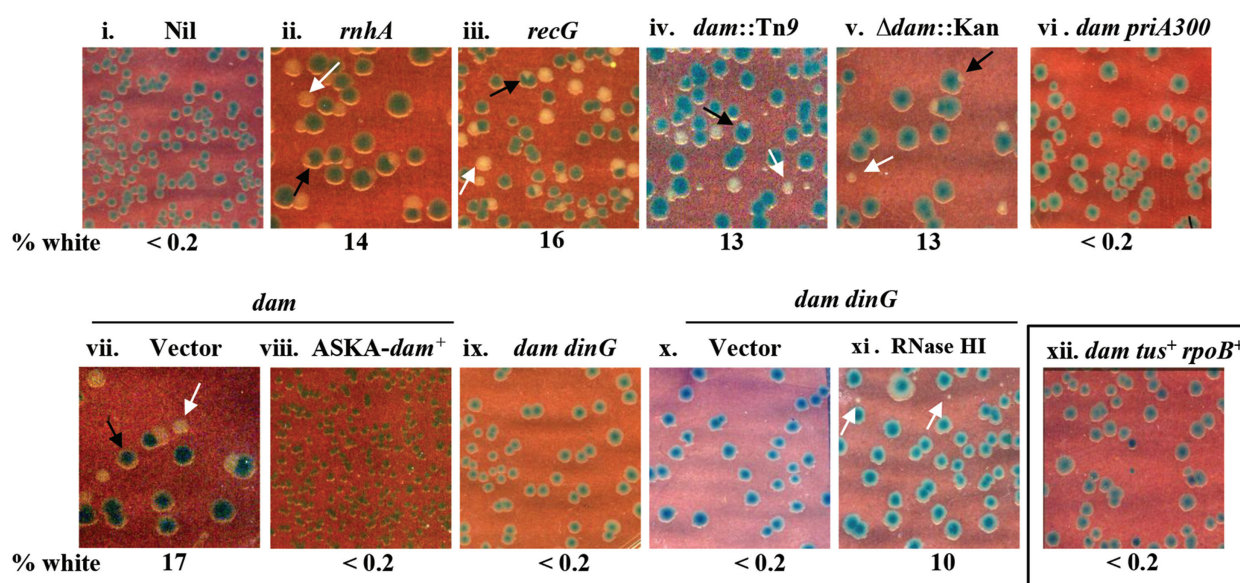
Figure 2. Perturbations that rescue Δ*dnaA* lethality. Isogenic Δ*dnaA* derivatives (also bearing *tus rpoB*35* mutations for all but that shown in panel xii) carrying *dnaA*+ shelter plasmid pHYD2388 (or pHYD4805, in case of *recG* mutant) and the additional genetic perturbation(s) as indicated on the top of each panel were plated on LB-Xgal plates and incubated for 40 hours at 37°; representative images are shown, and the numbers beneath each of the panels indicate the percentage of white colonies to the total, that is, viable even in absence of *dnaA*+ shelter plasmid (minimum of 500 colonies counted). Examples of white colonies and white-sectored blue colonies are marked by the white and black arrows, respectively. Strains employed for the different panels were pHYD2388 (or pHYD4805, in case of *recG* mutant) derivatives of: i, GJ16459; ii, GJ16475; iii, GJ16464; iv, GJ16445; v, GJ16488; vi, GJ18625; vii and viii, GJ16488 with pCA24N and pASKA-*dam*+, respectively; ix, GJ16469; x, GJ18626; xi, GJ18613; and xii, GJ18628. The medium was supplemented with Ara at 0.2% for panels x and xi.

since the combination of *dam rpoB*35*, even when *dnaA*+, grows poorly on minimal medium. As expected, the occurrence of white colonies (as an indicator of Δ*dnaA* viability) was accompanied also by presence of white-sectored blue colonies on the plates (see Figure 2 and Supplementary Figure S4B). Rescue of Δ*dnaA* lethality was abolished also upon introduction into these derivatives of a plasmid with the cloned *dam*+ gene but not of the vector alone (Figure 2, compare panels vii and viii), indicating that the phenotype was not being conferred by any additional mutations that may have arisen in the *dam* strain, which is known to have a mutator phenotype (5,8).

Roles for DinG and PriA in rescue of Δ*dnaA* lethality by *dam*

The DinG helicase is required for overcoming the effects of major head-on transcription-replication conflicts in *E. coli*, as evidenced by the fact that *dinG* derivatives with one or more of the *rrn* operons in inverted orientation are unable to grow on rich medium; most interestingly, this growth defect is suppressed by RNase H overexpression, with the implication that growth-inhibitory R-loops are being formed at sites of strong transcription–replication conflict (58). Other recent studies have also pointed to R-loop formation as a contributor to the deleterious effects of head-on collisions on the DNA template between transcription and replication machineries (33,59,60), but the underlying mechanism remains unclear (61). Since retrograde fork progression in cSDR is expected to generate conflicts between the replisome and *rrn* transcription, we examined the role of DinG on rescue of Δ*dnaA* lethality in the *dam* mutant.

Introduction of Δ*dinG* abolished the rescue of Δ*dnaA* lethality by the *dam* mutation (in the derivatives which also carried Δ*tus* and *rpoB*35*) (Figure 2, panel ix). As with the findings reported earlier for *dinG* and growth of strains with *rrn* operon inversions (58), Δ*dnaA* growth also was restored in the *dam* Δ*dinG* derivative upon Ara-induced RNase HI overexpression (Figure 2, compare panels x and xi for derivatives carrying, respectively, P*ara* alone or P*ara*-*rnhA*). Thus, RNase HI appears to play antagonistic roles in cSDR: its absence (in the *rnhA* mutant) promotes cSDR ostensibly through R-loop formation, and yet its overexpression also facilitates cSDR in certain situations by overcoming the deleterious consequences of transcription-replication conflict.

The PriA protein, that is crucial for DnaA-independent replication initiation from D-loops and R-loops as well as for restart from intact but inactivated or disintegrated replication forks, has also earlier been shown to be required for cSDR (17). The *priA300* mutation, encoding a K230R substitution which abolishes the 3'-5' DNA helicase activity of the protein, abolishes rescue by *recG* of lethality associated with DnaA deficiency (25), and that by *rnhA* in some situations (26). We found in this study that the effect of *dam* mutation in restoring viability to Δ*dnaA tus rpoB*35* is also suppressed upon introduction of the *priA300* mutation (Figure 2, panel vi).

Absence of association between SeqA and cSDR

SeqA binds to DNA that is hemi-methylated at GATC sites, and hence the loss of methylation in Dam-deficient strains would lead to an abrogation of SeqA functions (62,63).

Given that Δ*dam* conferred viability to Δ*dnaA* (in presence of Δ*tus* and *rpoB*35*), we tested the role if any of SeqA on cSDR. Δ*seqA* by itself was unable to confer viability to the Δ*dnaA* derivative (Supplementary Figure S1, panel iv), nor was the rescue of Δ*dnaA* lethality by *dam* abolished by mutation in *seqA* (Supplementary Figure S1, panel v).

DSEs in *dam* mutant contribute to its cSDR phenotype

As mentioned above, Dam deficiency is associated also with occurrence of DSEs in the genome that are generated by action of the proteins MutHLS of methyl-directed mismatch repair (7,8). Rescue of Δ*dnaA* lethality by *dam* on LB medium was abolished by mutations in the *mutH/L/S* genes of mismatch repair (Figure 3A, compare panel i with panels ii–iv). The phenotype was complementable, that is, Δ*dnaA* viability was restored in the *dam mutS* mutant carrying *mutS*[+] in *trans* (Figure 3A, panel v) demonstrating once again that no incidental suppressor mutation had arisen in these derivatives. These results suggest that DSEs are required for conferring robust Δ*dnaA* viability in the *dam* strains.

Other perturbations that generate DSEs do not rescue Δ*dnaA* inviability

Since our findings above had implicated DSEs in the Δ*dam* mutant as being required for rescue of Δ*dnaA* viability, we tested whether other perturbations (DNA-damaging agents, or mutations) that increase DSE frequency would also confer viability in the Δ*dnaA* Δ*tus rpoB*35* derivatives. As with *dam*, the mutations are also associated with a hyper-recombination phenotype and synthetic lethality with mutations affecting recombinational repair or replication restart (64,65).

However, none of the perturbations tested, which included exposure to sublethal concentrations of phleomycin, bleomycin, norfloxacin, ciprofloxacin, 2-aminopurine, or mitomycin C, was able to robustly rescue the Δ*dna*A lethality (Supplementary Figure S2, panels vi–xi). Furthermore, mutations in *rdgB* or *polA* which are expected to generate nicks in DNA that are converted to DSEs upon arrival of a succeeding replication fork (64–66), did not confer viability to Δ*dnaA* under these conditions (Supplementary Figure S2, panels iii–iv). A site-specific DSE generated by SbcCD-mediated cleavage of a long palindromic sequence inserted within the *lacZ* gene (29) was also not proficient in conferring viability to the Δ*dnaA tus rpoB*35* cells (Supplementary Figure S2, panel v).

Phleomycin can rescue Δ*dnaA* lethality in the *dam* Δ*mutS* background

Given the observations that DSEs are needed for rescue of Δ*dnaA* lethality in the *dam* mutant, but that other perturbations which generate DSEs do not appear to rescue such lethality, we considered the possibility that there is a second property in the *dam* strain, in addition to DSE formation, that is required for cSDR. This idea was supported by our finding that addition of phleomycin (at 1 μg/ml) could indeed suppress Δ*dnaA* lethality in a *dam* Δ*mutS* derivative

which also carried *tus* and *rpoB*35* mutations (Figure 3B, panel xi), under conditions in which there was no suppression in either the *dam*[+] *mut*[+] strain with phleomycin (Figure 3B, panel ix) or the *dam* Δ*mutS* strain without the genotoxin (Figure 3B, panel viii). The *dam*[+] Δ*mutS* strain also was lethal with Δ*dnaA*, both in absence and presence of phleomycin (Figure 3B, panels vii and x, respectively). The Δ*dnaA dam* Δ*mutS* cells remained viable only on medium supplemented with phleomycin and not in its absence (Figure 3C, middle row). Thus, Δ*dnaA* viability can be conferred by a combination of two perturbations (*dam* Δ*mutS*, and phleomycin), neither of which by itself is able to do so.

Copy number analysis of different chromosomal regions by deep sequencing in *dam dnaA*[+] and *dam* Δ*dnaA* derivatives

Asynchronously growing cultures of wild-type *E. coli* display a symmetrical gradient of copy numbers for the different regions around the circular chromosome, with the peak and the trough located near *oriC* and the terminus, respectively (13). Mutations in *rnhA*, *recG*, *topA* or the three exonucleases (that are associated with cSDR) confer a characteristic 'mid-terminus peak' that is superimposed on this gradient in *dnaA*[+] derivatives (19,20,25–27,34).

In similar copy number analysis experiments, the *dam dnaA*[+] derivative also exhibited a prominent mid-terminus peak (between *TerA* and *TerC/B*), in comparison with the wild-type strain (Figure 4, compare panels i and ii); see also Supplementary Figure S3A, panels i and ii). The mid-terminus peak was absent in the *dam mutS* derivative (performed on two replicates which yielded identical profiles, one of which is shown in Figure 4, panel iii). As discussed below, these data provide support to our proposal (13) that the mid-terminus peak is a signature feature of cSDR and that, at least in case of the *dam* mutant, it is the result of replication forks progressing from stochastically distributed genome-wide supernumerary DNA replication initiation events. In presence of sublethal phleomycin (2 μg/ml), the wild-type strain itself exhibited a mid-terminus peak in the copy number analysis (Supplementary Figure S3A, panel iii).

It has previously been shown (25) that copy number profiles in the wild-type strain and its *tus rpoB*35* derivative are, as expected, identical (with peak at *oriC* and trough in the *TerA-TerC/B* interval). Most interestingly, we found that the *oriC* peak was lost in the *dam tus rpoB*35* or *dam rpoB*35* derivatives that were *dnaA*[+] (Figure 4, panels iv and v respectively), and that the copy number distributions across the genome were more or less flat in these strains (with only a small peak at the mid-terminus region). As further discussed below, we believe that this pattern is a reflection of the sum of aberrant replication initiation events in any individual *dam* mutant cell being equal to or exceeding the frequency of initiation from *oriC* itself.

In the viable Δ*dnaA* derivative of the *dam* mutant (carrying the additional *tus* and *rpoB*35* mutations), we confirmed loss of the *oriC* peak in the copy number analysis by deep sequencing (Figure 4, panel vi). Instead, a terminus-to-*oriC* gradient was observed [as has been described previously for *rnhA* (34) and *recG* (25) mutants in absence of DnaA function], which is also consistent with the model
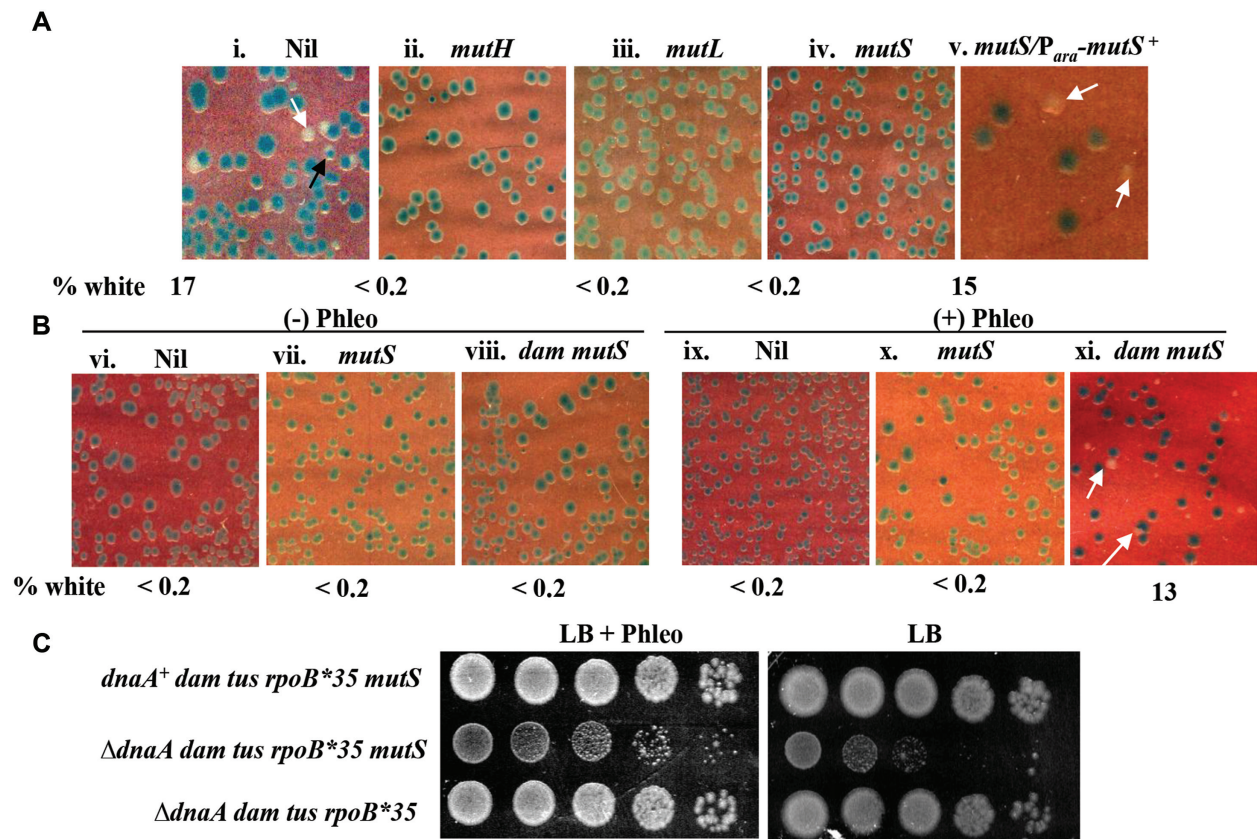
Figure 3. Roles of *dam* mutation and DSEs in rescue of Δ*dnaA* lethality. Isogenic derivatives of Δ*dnaA tus rpoB*35 dam*::Tn*9* (**A**) or Δ*dnaA tus rpoB*35* (**B**) strains carrying *dnaA*⁺ shelter plasmid pHYD2388 and the additional genetic and/or genotoxic perturbations as indicated on top of each panel were plated on LB-Xgal plates and incubated for 40 hours at 37°; representative images are shown, and the percentage of white colonies to total for each panel is indicated as explained in the legend to Figure 2. Strains employed for the different panels were pHYD2388 derivatives of: i, GJ16445; ii, GJ16438; iii, 18615; iv, viii, and xi, GJ16437; v, GJ16437/pHYD4807; vi and ix, GJ16459; and vii and x, GJ16427. Phleomycin (Phleo) supplementation for each of panels ix-xi was at 1 μg/ml, and with Ara for panel v at 0.2%. (**C**) Spotting assay at serial 10-fold dilutions to examine viability in presence (+) or absence (–) of phleomycin, for which the strains employed were (all *tus rpoB*35*, relevant genotypes indicated against each): top, GJ16437/pHYD2388; middle, GJ16437; and bottom, GJ16445. The top and middle rows represent blue and white colonies, respectively, from plate shown in Figure 3B, panel xi; and the bottom row represents a white colony from plate shown in Figure 3A, panel i.

proposed earlier of stochastic genome-wide cSDR initiation events (13).

The genome sequence data from the various strains also allowed us to verify their respective genotype status (such as Δ*dam*, Δ*tus*, *rpoB*35*, or Δ*mutS*). These data also served to exclude the possibility that in the Δ*dnaA* strains (which had been obtained following spontaneous loss of the shelter plasmid carrying the *S. enterica dnaA*⁺ gene), viability may have been the consequence of either (i) chromosomal integration of the *S. enterica dnaA*⁺ gene from the plasmid by homeologous recombination [which is known to occur when mismatch repair is compromised (67,68)], or (ii) mutation in *oriC* or any of the candidate genes conferring cSDR such as *rnhA*, *recG*, *topA*, *recJ* or any of the 3′-DNA exonucleases. Such confirmation was important, given that *dam* mutants exhibit an elevated frequency of spontaneous mutations (5,8); when compared with the parental strain, only one of the *dam* cultures (whose data are shown in Supplementary Figure S3A, panel ii) had no sequence changes, whereas each of the other cultures of *dam* derivatives harboured from 7 up to 18 additional single nucleotide polymorphisms (SNPs).

Rescue of Δ*dnaA* viability by *dam* occurs both in presence and absence of phi80 prophage

The DNA sequencing data had also indicated that the parental strain GJ13519 and all its derivatives including the *dam* and Δ*dnaA* mutants fortuitously bear the SOS-inducible prophage phi80 (see Supplementary Figure S3B), which is known to spread horizontally across strains in a laboratory environment (46,69,70). The copy number of phi80 genes in the wild-type strain was elevated ~4-fold upon SOS induction with sublethal phleomycin (Supplementary Figure S3B, compare panels i and iii). It was also increased in one of the two *dam* mutant cultures (Supplementary Figure S3B, elevated for culture in panel iv but not for that in panel ii); *dam* mutants have earlier been described to exhibit chronic SOS induction (71,72). In no instance was there copy number elevation of chromosomal genes flanking the prophage attachment sites, suggesting that the prophage was not a source of *oriC*-independent replication initiation for cSDR or iSDR.

To further test whether the prophage, or its induction, might in any way have contributed to rescue of Δ*dnaA*
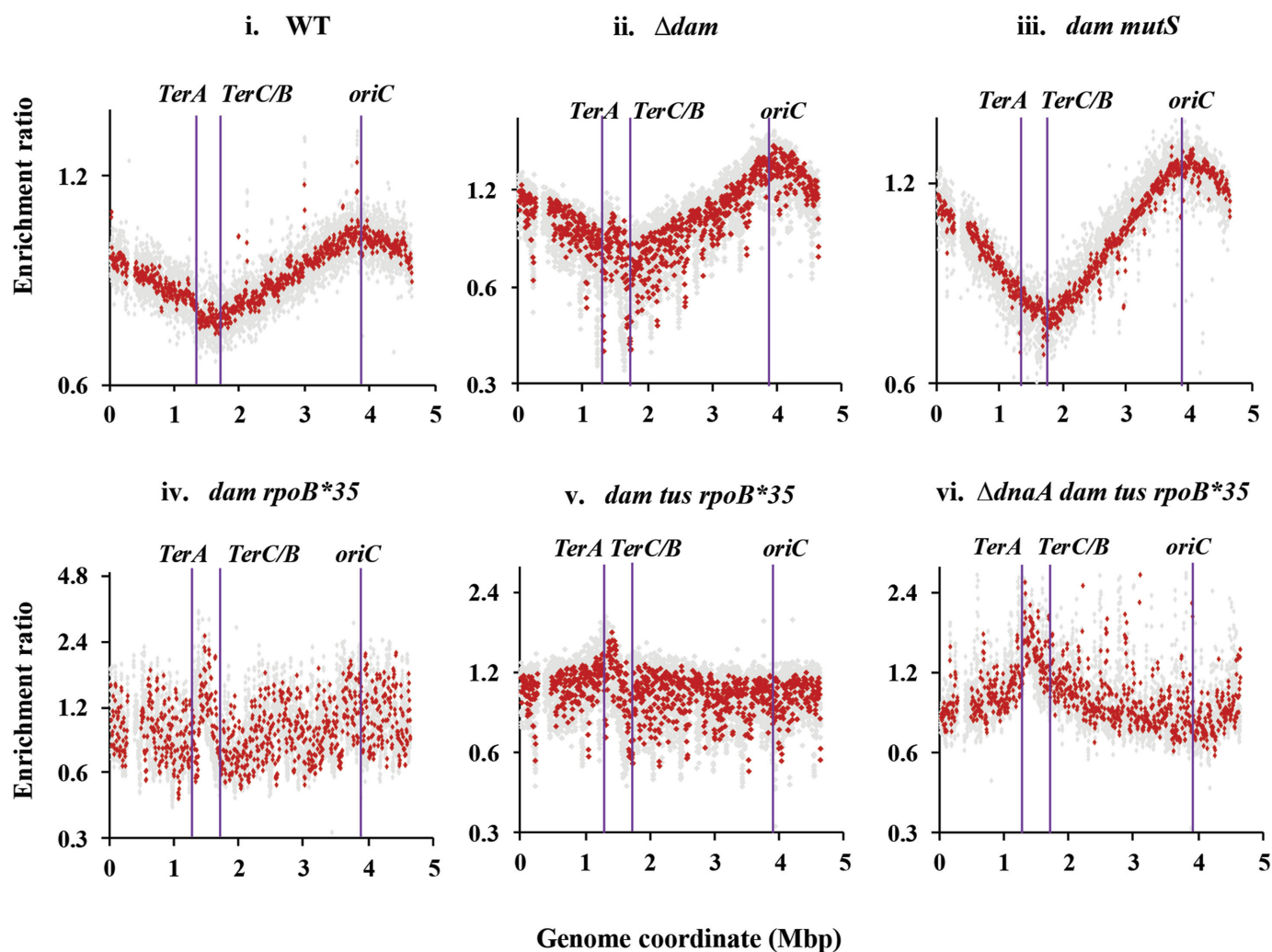
Figure 4. Copy number analysis by deep sequencing in *dam* mutants. From the sequencing reads for the indicated strains (grown to log phase in LB at 37°C), copy number distributions for 1-kb (gray) and overlapping 10-kb (red) intervals have been plotted on semi-log graphs as enrichment ratios across the genome, as described in the text and *Supplementary Text*. Positions of *oriC, TerA* and *TerC/B* are marked. The gap at around 0.3 Mb in each of the distribution plots corresponds to the *argF-lac* deletion present in the strains. Isogenic strains displayed in the different panels (their relevant genotypes indicated on top of each panel) are: i, GJ13519; ii, GJ18617; iii, GJ18618; iv, GJ16488; v, GJ16494; and vi, GJ18619/pHYD2388. WT, wild-type parent.

lethality by the *dam* mutation, we prepared derivatives of *tus rpoB*35* strains that were free of phi80 prophage and observed identical phenotypes in them (as that described above for the lysogenic strains) of: Δ*dnaA dam* viability which is abolished by *mutS* mutation, and Δ*dnaA dam mutS* viability (but not of Δ*dnaA dam⁺ mutS⁺*) in presence of phleomycin (Supplementary Figure S4B). We conclude that the presence or absence of phi80 prophage is immaterial to exhibition of the cSDR phenotypes associated with Dam deficiency.

Comparisons with cSDR in *rnhA* and *recG* mutants

As mentioned above, previous experiments to demonstrate the ability of *rnhA* or *recG* mutations to confer growth under DnaA-deficient conditions, have all employed strains carrying the temperature-sensitive *dnaA46* allele; hence the derivatives could be tested for growth only at the restrictive temperature (42°). Given our use of a Δ*dnaA* null allele in

this study, we have re-examined some of the cSDR features in *rnhA* and *recG* mutants.

The following additional novel properties of *rnhA*- and *recG*-mediated rescue of lethality associated with complete deficiency of DnaA were identified in these experiments. (i) It has previously been reported, from the experiments at 42°C, that DnaA-deficient *rnhA* is viable on minimal medium and that the *tus* and *rpoB*35* mutations are additionally needed for the derivatives to be viable on rich media (26). These results were confirmed in our experiments using Δ*dnaA*, but we found in addition that Δ*dnaA rnhA* (without *tus* or *rpoB*35*) is viable on LB medium at 30°C (Figure 5A). (ii) The Δ*dnaA rnhA* derivative was rendered viable on LB at 42°C upon introduction not only of *rpoB*35* as earlier reported (26) but also of a *sulA* mutation (Figure 5B), the latter indicating that Δ*dnaA rnhA* inviability is only because of SOS-induced hyper-filamentation under these conditions (73). Our microscopy experiments confirmed findings from earlier studies (17) that DnaA-deficient *rnhA* cells
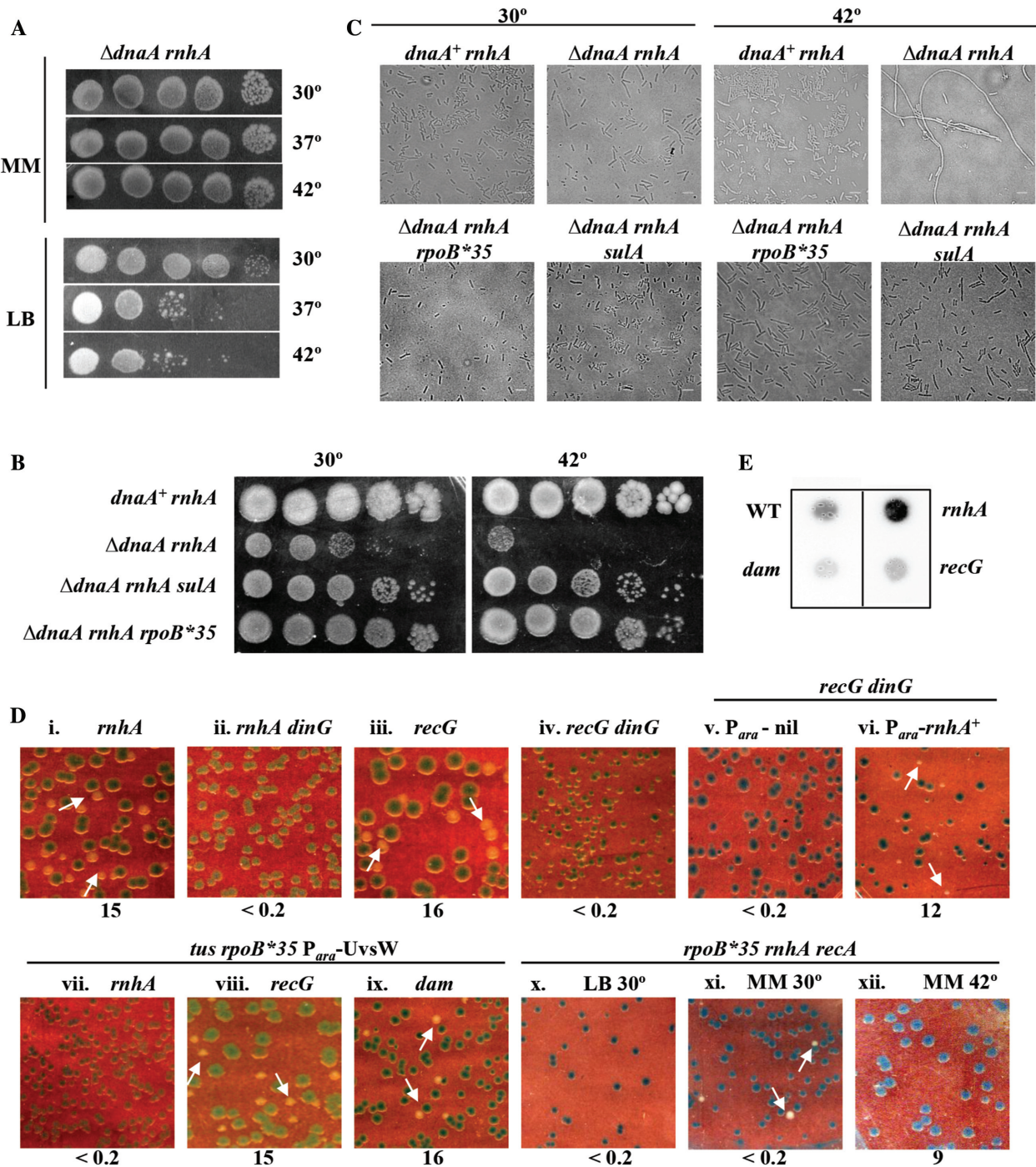
Figure 5. cSDR features in *rnhA* and *recG* mutants. Spotting at serial 10-fold dilutions, at the indicated temperatures, of suspensions of: (**A**) GJ16476 (Δ*dnaA rnhA*) on LB and glucose-minimal A (MM); and (**B**) in order, GJ16476/pHYD2388, GJ16476, GJ16498 and GJ18612 on LB. (**C**) Phase contrast microscopy of cultures of strains shown in panel B, after growth at 30°C or 42°C. Scale bar, 3 μm. (**D**) Plating of isogenic derivatives of Δ*dnaA* strain carrying *dnaA*+ shelter plasmid pHYD2388 and the additional genetic perturbation(s) as indicated on top of each panel on (unless otherwise indicated) LB-Xgal at 37°; representative images are shown, and the percentage of white colonies to total for each panel is indicated as explained in the legend to Figure 2. Strains employed for the different panels were pHYD2388 (or pHYD4805, in case of *recG* mutants) derivatives of: i, GJ16476; ii, GJ18620; iii, GJ16464; iv, GJ16489; v, GJ18621; vi, GJ18622; vii, GJ18623; viii, GJ16490; ix, GJ18627; and x-xii, GJ16499. Plates depicted in panels v–ix were supplemented with 0.2% arabinose. The plate of panel x was incubated at 30°C; while those of panels xi and xii comprised glucose-minimal A medium (MM) incubated at 30°C and 42°C, respectively. (**E**) Immunoblotting with S9.6 monoclonal antibody of total nucleic acids prepared from cultures of wild-type (WT) strain GJ13519 and its isogenic *rnhA*, *dam*, or *recG* derivatives GJ15833, GJ18617, and GJ17503, respectively.

are extremely filamented, and showed additionally that this is reversed by *sulA* or *rpoB*35* mutations (Figure 5C). (iii) As described above for *dam ΔdnaA tus rpoB*35*, so too the viability of *recG ΔdnaA tus rpoB*35*, and of *rnhA ΔdnaA* on LB, was lost upon introduction of the *ΔdinG* mutation (Figure 5D, compare panels i and iii with, respectively, ii and iv); this loss in the *recG* derivative was reversed once again with Ara-induced RNase HI overexpression (Figure 5D, compare panels v and vi). (Note that this experiment could not be attempted in the *rnhA* mutant, because of complementation of the *rnhA* defect itself under these conditions.) Furthermore, the *rnhA ΔdnaA dinG* derivative remained viable on glucose-minimal A (data not shown). (iv) In the *rnhA ΔdnaA* strain carrying *tus* and *rpoB*35* mutations, even RecA was dispensable for viability on glucose-minimal A medium at 30°C, but not so at 42°C nor even on LB at 30°C (Figure 5D, compare panels x–xii). As further discussed below, we interpret these data in terms of the quantitative threshold model introduced above for detecting cSDR-mediated rescue of *ΔdnaA* lethality, in which facilitatory roles are played by growth on minimal medium at 30° (as opposed to rich medium or 42°C), and by the *rpoB*35* and *tus* mutations.

Relationship between R-loops and cSDR

Finally, we examined the correlation if any between cSDR in the *rnhA*, *recG*, or *dam* mutants on the one hand, and R-loop abundance in them on the other. Kogoma (17) had earlier suggested that R-loops are responsible for cSDR in both *rnhA* and *recG* mutants, but their role in the case of *recG* has subsequently been questioned (25–29). In the *dam* mutants as well, we presumed that D-loops and not R-loops may be responsible for cSDR. The S9.6 monoclonal antibody (which is specific for RNA-DNA hybrids) has previously been used to demonstrate R-loop accumulation in different *E. coli* mutants (19,54); through a similar immunoblotting approach, we found that R-loop abundance (in comparison with that in the wild-type strain) is indeed elevated in the *rnhA* mutant [as has also been reported earlier (19)] but not so in the *recG* or *dam* mutants (Figure 5E). In a related observation, ectopic expression of the R-loop helicase UvsW also abolished rescue of *ΔdnaA* lethality by *rnhA* but not that by *recG* or *dam* mutations (Figure 5D, panels vii–ix).

DISCUSSION

Loss of function mutations that confer cSDR offer insights into mechanisms that otherwise act to prevent aberrant chromosomal replication in bacterial cells. RNase HI, RecG, topoisomerase I, and the single-strand DNA exonucleases have earlier been shown to play such a protective role, and in this work we have identified the Dam DNA methylase as yet another enzyme that is independently required for this purpose. A comparison between the various features of cSDR in the corresponding mutants is given in Supplementary Table S3. Our cSDR studies have also employed the more rigorous *ΔdnaA* mutation instead of the *dnaA46* temperature-sensitive allele that was used in the previous studies.

All the proteins above likely act in different ways to prevent abnormal *oriC*- and DnaA-independent replication

initiation; *ΔdnaA* viability under these conditions would of course be contingent on the replication forks successfully progressing to completion around the circular chromosome after overcoming both head-on collisions with transcription complexes (especially at *rrn* operons), and the trapping of forks in the terminus region. As explained below, we believe that a quantitative threshold model can account for many of the findings related to cSDR phenotypes, in both the present and earlier studies.

A quantitative threshold model to link cSDR with rescue of *ΔdnaA* lethality

Because, as stated above, of the problems faced by ectopically initiated replication forks to progress to completion around the chromosome (13), we propose a quantitative threshold model that links cSDR to the rescue of *ΔdnaA* lethality. Accordingly, *ΔdnaA* viability can be achieved either by having sufficiently large numbers of cSDR initiation events, or by fewer events in coordination with features or properties that facilitate the efficient retrograde progression (that is, towards *oriC*) of replication forks across the chromosome.

In our model, the facilitators for retrograde replication fork progression include the *rpoB*35* and *Δtus* mutations, DinG helicase (and in its absence RNase HI overexpression), growth on minimal medium, and low incubation temperature. The notion that high growth temperatures may be stressful for chromosomal replication might be in accord with the hypothesis of Pogliano and Beckwith (74), which posits a correlation between environmental conditions to which an essential physiological process may be sensitive and conditional phenotypes obtained with mutations affecting that process. The Pogliano-Beckwith model may additionally explain why the *sulA* mutation is required at 42°C but not at 30°C to allow *ΔdnaA rnhA* growth on rich medium, since cell division functions may also be considered as sub-optimal at elevated temperatures (75).

Two roles of *Δdam* in cSDR

At 37°C on LB medium, *dam* but not *dam ΔmutS* was able to suppress *ΔdnaA* lethality, suggesting that increased DSEs are needed for the suppression. On the other hand, sublethal phleomycin could suppress *ΔdnaA* lethality in the *dam ΔmutS* but not *dam*⁺ derivatives. Alterations of gene expression such as those caused by SOS induction, or by presence of *ΔdnaA* or *rpoB*35* mutations, cannot account for this difference, since they may be expected to have occurred to the same extent in both strains following phleomycin treatment. Therefore, the simplest hypothesis to explain these findings is that increased DSEs (generated either by MutHLS action in *Δdam* or by phleomycin in *dam*⁺) are necessary, but not sufficient, for rescue of *ΔdnaA* inviability; and that there is a second perturbation imposed by Dam deficiency (which is manifest even in the *dam mutS* strain) that is also required for the purpose.

In its first role, the *dam*-generated DSEs are expected to trigger break-induced DNA replication at the lesion sites, via formation of D-loops following the actions of recombinational repair proteins RecA, RecBCD, and RuvABC

(17,30,64). The likely second role for Δ*dam* in cSDR is not known, but our results indicate that this role does not involve SeqA. Since DSEs are clearly required for cSDR in the *dam* mutant, one may presume that the putative second role is in some way connected to replication restart.

It is possible that Dam may modulate replication restart indirectly, by affecting nucleoid structure or through transcriptional regulation of genes involved in the process. On the other hand, we would like to propose that Dam influences replication restart more directly, and that in *dam* mutants there is an increased likelihood of 'reverse restart', so that the newly assembled replisome is directed to proceed towards *oriC* instead of towards the terminus.

Different models have been put forth earlier for reverse restart-like mechanisms during Red-mediated recombination in phage λ (76) and in *E. coli recG* (24,29) or *recD* (77) mutants, any of which could apply in the *dam* mutant. The feature common to all of them, and which distinguishes them from normal replication restart, is that whereas in the latter there is one terminus-directed replisome that is assembled with the aid of PriABC and DnaT proteins following recombinational repair of a DSE, reverse restart results in a total of three replisomes, one directed towards *oriC* and two towards the terminus.

One such scheme for the *dam* mutant is outlined in Figure 6, which is based on the similar proposal earlier for *recG* (24,29). In this model, in absence of Dam methylation, the actions of PriA (including its helicase activity) in combination with those of PriB-DnaT or PriC lead to aberrant loading of the DnaB replicative helicase on the strand marked in red in panel C of Figure 6, so that the assembled replisome is now oriented for progression towards *oriC* (Figure 6, panel E). It is noteworthy in this context that the *priA300* allele (encoding helicase-deficient PriA) suppresses the rescue, in both *dam* (this study) and *recG* (25) mutants, of lethality caused by deficiency of DnaA. The other similarities between these two mutants for cSDR is also brought out in Supplementary Table S3.

If our model is correct, it remains to be investigated whether Dam methylation is needed for proper functioning of RecG (24,29), of PriA (78) or of both proteins in avoidance of reverse restart. The role postulated here for Dam in replication restart may also explain a curious finding from phylogenetic analyses that the Dam and PriB proteins have co-evolved, that is, different bacterial clades either possess the two proteins or they have neither (1,3).

Relationship between cSDR and occurrence of the mid-terminus peak in copy number analysis

The occurrence of peaks in chromosomal copy number distribution profiles is most often interpreted as origin sites for replication initiation, which has also been the case for mid-terminus peaks observed for the *rnhA*, *recG*, *topA* and the triple-exo mutants (19,20,25–27,34). On the other hand, we have earlier argued that whereas every origin (of finite strength) will be represented by a peak in the profile, the converse may not necessarily be true, especially for a peak in the mid-terminus region (13).

Thus the alternative model proposed for cSDR (13) suggests a genome-wide distribution of replication origins each of which fire stochastically at a very low frequency, with the mid-terminus peak being generated by algebraic summation of copy numbers from the different subpopulations of cells. A crucial contributory feature in this model is that when a replication fork is arrested at a Tus-bound *Ter* site for a significant period of time (that is, in the absence of its fusion with another fork coming in the opposite direction), there is
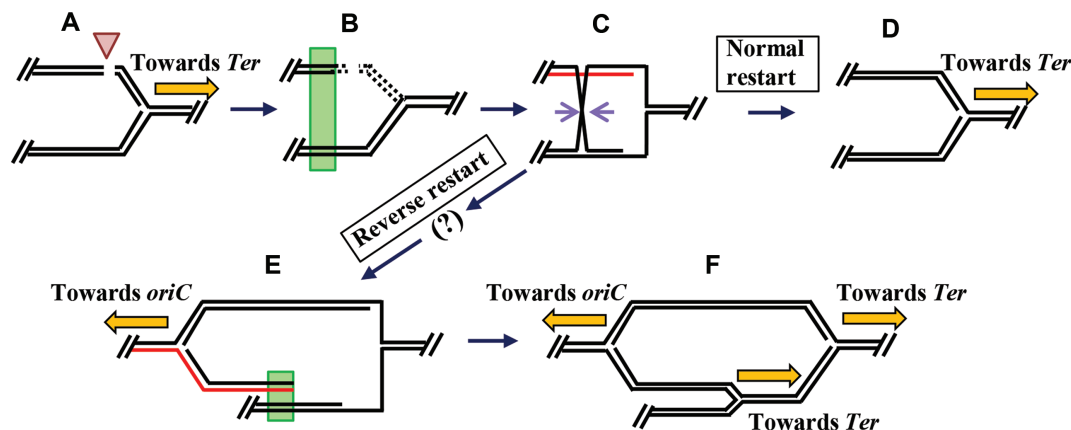
Figure 6. Model for a second role of *dam* in cSDR. (**A**) Shown schematically is a MutHLS-generated double strand break (arrowhead) in one of the daughter duplexes immediately behind a replisome that is progressing (ochre arrow) from *oriC* to *Ter* on the clockwise replichore in a *dam* mutant cell. (5′ to 3′ polarity for top strand in each of the duplexes is from left to right.) (**B**) Following RecBCD-mediated DNA degradation (shown by interrupted lines) from both ends of the break (64), the *ori*-proximal DSE that remains participates in repair by homologous recombination (green rectangle) with its sister duplex; alternatively (not shown), such recombination can occur also with a 'cousin' duplex (50,83). (**C**) One intermediate in the pathway of recombinational repair is shown, with the pair of mauve arrows marking sites of RuvC-mediated Holliday junction resolution. (**D**) Disposition of DNA strands following normal replication restart, with DnaB helicase (not shown) translocating from left to right on top strand of the parental duplex, towards *Ter*. (**E**) Disposition of DNA strands following reverse restart; PriA-mediated DnaB helicase loading is postulated to have occurred on strand shown in red (this panel, and panel C) with its translocation proceeding from right to left, towards *oriC*. The step shown by the question mark, in the progression from panel C to panel E, is to indicate that the intermediates in the reverse restart pathway are at present undefined. (**F**) Disposition of DNA strands and of three replisomes following homologous recombination (at site marked by green rectangle in panel E) and normal restart, similar to pathway depicted in panels B through D.

marked degradation of DNA proximal to the arrest site; this element of the model is strongly supported by data from a large number of earlier studies on strains with ectopic replication origins or ectopic *Ter* sites (13,25,27,79,80).

Rudolph and coworkers (51) have also recently shown that for a triple-*ori* strain (that is, with native *oriC* and two additional *oriC* sequences ectopically positioned in the two replichores), the copy number profile comprises not only the three *ori*-associated peaks but also a mid-terminus peak. For the latter, they have proposed a similar model as discussed above, of copy number summation from different subpopulations in the culture.

Hence the finding in this work of a mid-terminus peak in the Δ*dam* mutant is consistent with the model of genome-wide distribution of stochastically firing replication origins, coupled with DNA degradation proximal to forks arrested at *Ter* sites (13). We believe it unlikely that the *dam* mid-terminus peak itself represents a site of replication initiation. The fact that a similar peak is seen also in the wild-type strain grown with sublethal doses of phleomycin (Supplementary Figure S3A, panel iii), suggests that such distributed sites of replication initiation occur under these conditions as well. These results, as well as those from flow cytometry in Figure 1A, point to the close relationship between cSDR and iSDR, as had initially been proposed by Kogoma (17).

Can replication initiation triggered genome-wide by Dam deficiency exceed that from *oriC*?

It is also remarkable from the copy number analyses that the *oriC* peak, and bidirectional gradient therefrom, in a *dnaA+ dam* mutant during log-phase growth is almost completely abolished in derivatives that additionally carry the *rpoB*35* or *tus rpoB*35* mutations. We propose that the reason for flattening of the gradient in the latter two strains is because the true strength of the stochastically distributed cSDR origins in the *dam* mutant is revealed only when the problems of fork progression across the chromosome are alleviated (by *tus* and *rpoB*35*). Consequently, there is now little difference in copy number distributions between the *dnaA+* and Δ*dnaA* derivatives of the *dam tus rpoB*35* strains (compare panels v and vi in Figure 4); and the patterns in both are indeed reminiscent of that in the *Haloferax volcanii* mutant in which replication initiation was postulated to occur from widely distributed origins following site-specific deletion of its four discrete *ori* sequences (81).

RecA and cSDR

For cSDR and rescue of Δ*dnaA* lethality, one can conceive of multiple roles of RecA (17,64,73), including in (i) generation of substrates for aberrant replication initiation, (ii) direct recombinational repair following problems of transcription-replication conflict or of fork breakage at Tus-bound *Ter* sites, and (iii) SOS induction (of genes such as UvrD that are also involved in taking care of such problems). Earlier work had indicated that cSDR in both *rnhA* and *recG* mutants is abolished by *recA* mutation (17,25,26), and it was suggested that the formation of, respectively, R-loops and D-loops for replication initiation in the two cases required RecA function.

Against this scenario, it is indeed remarkable that our present work has demonstrated rescue of Δ*dnaA* lethality (at 30°C) even in presence of *recA* mutation in the *rnhA* mutant. This finding is consistent with recent models that transcription-associated R-loop formation is RecA-independent (82). The features of the quantitative threshold model may also be important here, in that an absence of RecA may simply reduce the likelihood of successful completion of DnaA-independent replication in the mutants.

DATA AVAILABILITY

The genome sequence data from this work are available at https://www.ncbi.nlm.nih.gov/bioproject/PRJNA513325.

SUPPLEMENTARY DATA

Supplementary Data are available at NAR Online.

REFERENCES

1. Løbner-Olesen,A., Skovgaard,O. and Marinus,M.G. (2005) Dam methylation: coordinating cellular processes. *Curr. Opin. Microbiol.*, **8**, 154–160.
2. Wion,D. and Casadesús,J. (2006) N6-methyl-adenine: an epigenetic signal for DNA-protein interactions. *Nat. Rev. Microbiol.*, **4**, 183–192.
3. Marinus,M.G. and Løbner-Olesen,A. (2014) DNA methylation. *EcoSal Plus*, **14**, 517–548.
4. Marinus,M.G. and Morris,N.R. (1973) Isolation of deoxyribonucleic acid methylase mutants of *Escherichia coli* K-12. *J. Bacteriol.*, **114**, 1143–1150.
5. Marinus,M.G. and Morris,N.R. (1974) Biological function for 6-methyladenine residues in the DNA of *Escherichia coli* K-12. *J. Mol. Biol.*, **85**, 309–322.
6. Putnam,C.D. (2016) Evolution of the methyl directed mismatch repair system in *Escherichia coli*. *DNA Repair (Amst).*, **38**, 32–41.

7. McGraw,B.R. and Marinus,M.G. (1980) Isolation and characterization of Dam$^+$ revertants and suppressor mutations that modify secondary phenotypes of *dam*-3 strains of *Escherichia coli* K-12. *Mol. Gen. Genet.*, **178**, 309–315.

8. Glickman,B.W. and Radman,M. (1980) *Escherichia coli* mutator mutants deficient in methylation-instructed DNA mismatch correction. *Proc. Natl. Acad. Sci. U.S.A.*, **77**, 1063–1067.

9. Au,K.G., Welsh,K. and Modrich,P. (1992) Initiation of methyl-directed mismatch repair. *J. Biol. Chem.*, **267**, 12142–12148.

10. Marinus,M.G. (2000) Recombination is essential for viability of an *Escherichia coli dam* (DNA adenine methyltransferase) mutant. *J. Bacteriol.*, **182**, 463–468.

11. Harinarayanan,R. and Gowrishankar,J. (2004) A *dnaC* mutation in *Escherichia coli* that affects copy number of Co1E1-like plasmids and the PriA-PriB (but not Rep-PriC) pathway of chromosomal replication restart. *Genetics*, **166**, 1165–1176.

12. O'Donnell,M., Langston,L. and Stillman,B. (2013) Principles and concepts of DNA replication in bacteria, archaea, and eukarya. *Cold Spring Harb. Perspect. Biol.*, **5**, a010108.

13. Gowrishankar,J. (2015) End of the beginning: elongation and termination features of alternative modes of chromosomal replication initiation in bacteria. *PLos Genet.*, **11**, e1004909.

14. Neylon,C., Kralicek,A. V, Hill,T.M. and Dixon,N.E. (2005) Replication termination in *Escherichia coli*: structure and antihelicase activity of the Tus- Ter complex. *Microbiol. Mol. Biol. Rev.*, **69**, 501–526.

15. Duggin,I.G., Wake,R.G., Bell,S.D. and Hill,T.M. (2008) The replication fork trap and termination of chromosome replication. *Mol. Microbiol.*, **70**, 1323–1333.

16. Kaplan,D.L. and Bastia,D. (2009) Mechanisms of polar arrest of a replication fork. *Mol. Microbiol.*, **72**, 279–285.

17. Kogoma,T. (1997) Stable DNA replication: interplay between DNA replication, homologous recombination, and transcription. *Microbiol. Mol. Biol. Rev.*, **61**, 212–238.

18. Martel,M., Balleydier,A., Sauriol,A. and Drolet,M. (2015) Constitutive stable DNA replication in *Escherichia coli* cells lacking type 1A topoisomerase activity. *DNA Repair (Amst).*, **35**, 37–47.

19. Brochu,J., Vlachos-Breton,É., Sutherland,S., Martel,M. and Drolet,M. (2018) Topoisomerases I and III inhibit R-loop formation to prevent unregulated replication in the chromosomal Ter region of *Escherichia coli. PLos Genet.*, **14**, e1007668.

20. Midgley-Smith,S.L., Dimude,J.U. and Rudolph,C.J. (2019) A role for 3′ exonucleases at the final stages of chromosome duplication in *Escherichia coli. Nucleic Acids Res.*, **47**, 1847–1860.

21. Cox,M.M., Goodman,M.F., Kreuzer,K.N., Sherratt,D.J., Sandler,S.J. and Marians,K.J. (2000) The importance of repairing stalled replication forks. *Nature*, **404**, 37–41.

22. Windgassen,T.A., Wessel,S.R., Bhattacharyya,B. and Keck,J.L. (2018) Mechanisms of bacterial DNA replication restart. *Nucleic Acids Res.*, **46**, 504–519.

23. Michel,B. and Sandler,S.J. (2017) Replication restart in bacteria. *J. Bacteriol.*, **199**, e00102-17.

24. Michel,B., Sinha,A.K. and Leach,D.R.F. (2018) Replication fork breakage and restart in *Escherichia coli. Microbiol. Mol. Biol. Rev.*, **82**, e00013-18.

25. Rudolph,C.J., Upton,A.L., Stockum,A., Nieduszynski,C.A. and Lloyd,R.G. (2013) Avoiding chromosome pathology when replication forks collide. *Nature*, **500**, 608–611.

26. Dimude,J.U., Stockum,A., Midgley-Smith,S.L., Upton,A.L., Foster,H.A., Khan,A., Saunders,N.J., Retkute,R. and Rudolph,C.J. (2015) The consequences of replicating in the wrong orientation: bacterial chromosome duplication without an active replication origin. *MBio*, **6**, e01294-15.

27. Midgley-Smith,S.L., Dimude,J.U., Taylor,T., Forrester,N.M., Upton,L., Lloyd,R.G. and Rudolph,C.J. (2018) Chromosomal over-replication in *Escherichia coli recG* cells is triggered by replication fork fusion and amplified if replichore symmetry is disturbed. *Nucleic Acids Res.*, **46**, 7701–7715.

28. Wendel,B.M., Courcelle,C.T. and Courcelle,J. (2014) Completion of DNA replication in *Escherichia coli. Proc. Natl. Acad. Sci. U.S.A.*, **111**, 16454–16459.

29. Azeroglu,B., Mawer,J.S.P., Cockram,C.A., White,M.A., Hasan,A.M.M., Filatenkova,M. and Leach,D.R.F. (2016) RecG directs DNA synthesis during double-strand break Repair. *PLos Genet.*, **12**, e1005799.

30. Anand,R.P., Lovett,S.T. and Haber,J.E. (2013) Break-induced DNA replication. *Cold Spring Harb. Perspect. Biol.*, **5**, a010397.

31. McGlynn,P. and Lloyd,R.G. (2000) Modulation of RNA polymerase by (p)ppGpp reveals a RecG-dependent mechanism for replication fork progression. *Cell*, **101**, 35–45.

32. Trautinger,B.W., Jaktaji,R.P., Rusakova,E. and Lloyd,R.G. (2005) RNA polymerase modulators and DNA repair activities resolve conflicts between DNA replication and transcription. *Mol. Cell*, **19**, 247–258.

33. Dutta,D., Shatalin,K., Epshtein,V., Gottesman,M.E. and Nudler,E. (2011) Linking RNA polymerase backtracking to genome instability in E. coli. *Cell*, **146**, 533–543.

34. Maduike,N.Z., Tehranchi,A.K., Wang,J.D. and Kreuzer,K.N. (2014) Replication of the *Escherichia coli* chromosome in RNase HI-deficient cells: multiple initiation regions and fork dynamics. *Mol. Microbiol.*, **91**, 39–56.

35. Miller,J.H. (1992) *A Short Course in Bacterial Genetics: A Laboratory Manual and Handbook for Escherichia coli and Related Bacteria*. Cold Spring Harbor Lab Press, NY.

36. Anupama,K., Leela,J.K. and Gowrishankar,J. (2011) Two pathways for RNase E action in *Escherichia coli* in vivo and bypass of its essentiality in mutants defective for Rho-dependent transcription termination. *Mol. Microbiol.*, **82**, 1330–1348.

37. Baba,T., Ara,T., Hasegawa,M., Takai,Y., Okumura,Y., Baba,M., Datsenko,K.A., Tomita,M., Wanner,B.L. and Mori,H. (2006) Construction of *Escherichia coli* K-12 in-frame, single-gene knockout mutants: the Keio collection. *Mol. Syst. Biol.*, **2**, doi:10.1038/msb4100050.

38. Datsenko,K.A. and Wanner,B.L. (2000) One-step inactivation of chromosomal genes in *Escherichia coli* K-12 using PCR products. *Proc. Natl. Acad. Sci. U.S.A.*, **97**, 6640–6645.

39. Guzman,L.M., Belin,D., Carson,M.J. and Beckwith,J. (1995) Tight regulation, modulation, and high-level expression by vectors containing the arabinose P$_{BAD}$ promoter. *J. Bacteriol.*, **177**, 4121–4130.

40. Andrews,A.E., Lawley,B. and Pittard,A.J. (1991) Mutational analysis of repression and activation of the *tyrP* gene in *Escherichia coli. J. Bacteriol.*, **173**, 5068–5078.

41. Kitagawa,M., Ara,T., Arifuzzaman,M., Ioka-Nakamichi,T., Inamoto,E., Toyonaga,H. and Mori,H. (2005) Complete set of ORF clones of *Escherichia coli* ASKA library (*A* complete *S*et of *E. coli K*-12 ORF *A*rchive): unique resources for biological research. *DNA Res.*, **12**, 291–299.

42. Galli,E., Midonet,C., Paly,E. and Barre,F.-X. (2017) Fast growth conditions uncouple the final stages of chromosome segregation and cell division in *Escherichia coli. PLos Genet.*, **13**, e1006702.

43. Gowrishankar,J. (1985) Identification of osmoresponsive genes in *Escherichia coli*: evidence for participation of potassium and proline transport systems in osmoregulation. *J. Bacteriol.*, **164**, 434–445.

44. Sambrook,J. and Russell,D. (2001) *Molecular Cloning: A Laboratory Manual*. 3rd edn. Cold Spring Harbor Lab Press, NY.

45. Harinarayanan,R. and Gowrishankar,J. (2003) Host factor titration by chromosomal R-loops as a mechanism for runaway plasmid replication in transcription termination-defective mutants of *Escherichia coli. J. Mol. Biol.*, **332**, 31–46.

46. Harms,A., Fino,C., Sørensen,M.A., Semsey,S. and Gerdes,K. (2017) Prophages and growth dynamics confound experimental results with antibiotic-tolerant persister cells. *MBio*, **8**, e01964-17.

47. Boyd,D., Weiss,D.S., Chen,J.C. and Beckwith,J. (2000) Towards single-copy gene expression systems making gene cloning physiologically relevant: Lambda InCh, a simple *Escherichia coli* plasmid-chromosome shuttle system. *J. Bacteriol.*, **182**, 842–847.

48. Roberts,D., Hoopes,B.C., McClure,W.R. and Kleckner,N. (1985) IS10 transposition is regulated by DNA adenine methylation. *Cell*, **43**, 117–130.

49. del Solar,G., Giraldo,R., Ruiz-Echevarría,M.J., Espinosa,M. and Díaz-Orejas,R. (1998) Replication and control of circular bacterial plasmids. *Microbiol. Mol. Biol. Rev.*, **62**, 434–464.

50. Khan,S.R., Mahaseth,T., Kouzminova,E.A., Cronan,G.E. and Kuzminov,A. (2016) Static and dynamic factors limit chromosomal replication complexity in *Escherichia coli*, avoiding dangers of runaway overreplication. *Genetics*, **202**, 945–960.

51. Dimude,J.U., Stein,M., Andrzejewska,E.E., Khalifa,M.S., Gajdosova,A., Retkute,R., Skovgaard,O. and Rudolph,C.J. (2018) Origins left, right, and centre: increasing the number of initiation sites in the *Escherichia coli* chromosome. *Genes*, **9**, 5–7.

52. Martel,M., Balleydier,A., Brochu,J. and Drolet,M. (2018) Detection of *oriC* independent replication in *Escherichia coli* Cells. In: Drolet,M (eds). *DNA Topoisomerases. Methods in Molecular Biology*, Humana Press, NY, Vol. **1703**, pp. 131–138.

53. Espeli,O., Mercier,R. and Boccard,F. (2008) DNA dynamics vary according to macrodomain topography in the *E. coli* chromosome. *Mol. Microbiol.*, **68**, 1418–1427.

54. Raghunathan,N., Kapshikar,R.M., Leela,J.K., Mallikarjun,J., Bouloc,P. and Gowrishankar,J. (2018) Genome-wide relationship between R-loop formation and antisense transcription in *Escherichia coli*. *Nucleic Acids Res.*, **46**, 3400–3411.

55. Sivaramakrishnan,P., Sepúlveda,L.A., Halliday,J.A., Liu,J., Núñez,M.A.B., Golding,I., Rosenberg,S.M. and Herman,C. (2017) The transcription fidelity factor GreA impedes DNA break repair. *Nature*, **550**, 214–218.

56. Bhattacharyya,S., Soniat,M.M., Walker,D., Jang,S., Finkelstein,I.J. and Harshey,R.M. (2018) Phage Mu Gam protein promotes NHEJ in concert with *Escherichia coli* ligase. *Proc. Natl. Acad. Sci. U.S.A.*, **115**, E11614–E11622.

57. Leela,J.K., Syeda,A.H., Anupama,K. and Gowrishankar,J. (2013) Rho-dependent transcription termination is essential to prevent excessive genome-wide R-loops in *Escherichia coli*. *Proc. Natl. Acad. Sci. U.S.A.*, **110**, 258–263.

58. Boubakri,H., de Septenville,A.L., Viguera,E. and Michel,B. (2010) The helicases DinG, Rep and UvrD cooperate to promote replication across transcription units in vivo. *EMBO J.*, **29**, 145–157.

59. Lang,K.S., Hall,A.N., Merrikh,C.N., Ragheb,M., Tabakh,H., Pollock,A.J., Woodward,J.J., Dreifus,J.E. and Merrikh,H. (2017) Replication-transcription conflicts generate R-loops that orchestrate bacterial stress survival and pathogenesis. *Cell*, **170**, 787–799.

60. Zhang,Y., Mooney,R.A., Grass,J.A., Sivaramakrishnan,P., Herman,C., Landick,R. and Wang,J.D. (2014) DksA guards elongating RNA polymerase against ribosome-stalling-induced arrest. *Mol. Cell*, **53**, 766–778.

61. Kuzminov,A. (2018) When DNA topology turns deadly - RNA polymerases dig in their R-Loops to stand their ground: new positive and negative (super)twists in the replication-transcription conflict. *Trends Genet.*, **34**, 111–120.

62. Lu,M., Campbell,J.L., Boye,E. and Kleckner,N. (1994) SeqA: A negative modulator of replication initiation in E. coli. *Cell*, **77**, 413–426.

63. Løbner-Olesen,A., Marinus,M.G. and Hansen,F.G. (2003) Role of SeqA and Dam in *Escherichia coli* gene expression: a global/microarray analysis. *Proc. Natl. Acad. Sci. U.S.A.*, **100**, 4672–4677.

64. Kuzminov,A. (1999) Recombinational repair of DNA damage in *Escherichia coli* and bacteriophage lambda. *Microbiol. Mol. Biol. Rev.*, **63**, 751–813.

65. Kouzminova,E.A., Rotman,E., Macomber,L., Zhang,J. and Kuzminov,A. (2004) RecA-dependent mutants in *Escherichia coli* reveal strategies to avoid chromosomal fragmentation. *Proc. Natl. Acad. Sci. USA*, **101**, 16262–16267.

66. Kuzminov,A. (1995) Collapse and repair of replication forks in *Escherichia coli*. *Mol. Microbiol.*, **16**, 373–384.

67. Rayssiguier,C., Thaler,D.S. and Radman,M. (1989) The barrier to recombination between *Escherichia coli* and *Salmonella typhimurium* is disrupted in mismatch-repair mutants. *Nature*, **342**, 189–192.

68. Matic,I., Rayssiguier,C. and Radman,M. (1995) Interspecies gene exchange in bacteria: The role of SOS and mismatch repair systems in evolution of species. *Cell*, **80**, 507–515.

69. Rotman,E., Amado,L. and Kuzminov,A. (2010) Unauthorized horizontal spread in the laboratory environment: The tactics of Lula, a temperate lambdoid bacteriophage of *Escherichia coli*. *PLoS One*, **5**, e11106.

70. Rotman,E., Kouzminova,E., Plunkett,G. and Kuzminov,A. (2012) Genome of enterobacteriophage lula/phi80 and insights into its ability to spread in the laboratory environment. *J. Bacteriol.*, **194**, 6802–6817.

71. Saisree,L., Reddy,M. and Gowrishankar,J. (2000) *lon* incompatibility associated with mutations causing SOS induction: null *uvrD* alleles induce an SOS response in *Escherichia coli*. *J. Bacteriol.*, **182**, 3151–3157.

72. McCool,J.D., Long,E., Petrosino,J.F., Sandler,H.A., Rosenberg,S.M. and Sandler,S.J. (2004) Measurement of SOS expression in individual *Escherichia coli* K-12 cells using fluorescence microscopy. *Mol. Microbiol.*, **53**, 1343–1357.

73. Simmons,L.A., Foti,J.J., Cohen,S.E. and Walker,G.C. (2013) The SOS regulatory network. *EcoSal Plus*, doi:10.1128/ecosalplus.5.4.3.

74. Pogliano,K.J. and Beckwith,J. (1993) The Cs sec mutants of *Escherichia coli* reflect the cold sensitivity of protein export itself. *Genetics*, **133**, 763–773.

75. Blaauwen,T. Den, Hamoen,L.W. and Levin,P.A. (2017) The divisome at 25:the road ahead. *Curr. Opin. Microbiol.*, **36**, 85–94.

76. Skalka,A. (1974) A replicator`s view of recombination (and repair). In: Grell,R (ed). *Mechanisms in Recombination*. Springer US, Boston, MA, pp. 421–432.

77. White,M.A., Azeroglu,B., Lopez-Vernaza,M.A., Hasan,A.M.M. and Leach,D.R.F. (2018) RecBCD coordinates repair of two ends at a DNA double-strand break, preventing aberrant chromosome replication. *Nucleic Acids Res.*, **46**, 6670–6682.

78. Windgassen,T.A., Leroux,M., Satyshur,K.A., Sandler,S.J. and Keck,J.L. (2018) Structure-specific DNA replication-fork recognition directs helicase and replication restart activities of the PriA helicase. *Proc. Natl. Acad. Sci. U.S.A.*, **115**, 9075–9084.

79. Levy,A., Goren,M.G., Yosef,I., Auster,O., Manor,M., Amitai,G., Edgar,R., Qimron,U. and Sorek,R. (2015) CRISPR adaptation biases explain preference for acquisition of foreign DNA. *Nature*, **520**, 505–510.

80. Ivanova,D., Taylor,T., Smith,S.L., Dimude,J.U., Upton,A.L., Mehrjouy,M.M., Skovgaard,O., Sherratt,D.J., Retkute,R. and Rudolph,C.J. (2015) Shaping the landscape of the *Escherichia coli* chromosome: replication-transcription encounters in cells with an ectopic replication origin. *Nucleic Acids Res.*, **43**, 7865–7877.

81. Hawkins,M., Malla,S., Blythe,M.J., Nieduszynski,C.A. and Allers,T. (2013) Accelerated growth in the absence of DNA replication origins. *Nature*, **503**, 544–547.

82. Gowrishankar,J., Leela,J.K. and Anupama,K. (2013) R-loops in bacterial transcription. *Transcription*, **4**, 153–157.

83. Kuzminov,A. (2016) Chromosomal replication complexity: a novel DNA metrics and genome instability factor. *PLos Genet.*, **12**, e1006229.